SiliconPV: March 25-27, 2013, Hamelin, Germany

Considering the distributed series resistance in a two-diode model

Sven Rißland*, Otwin Breitenstein

Max Planck Institute of Microstructure Physics, Weinberg 2, 06120 Halle, Gemany

Abstract

The interpretation of the global current-voltage (*I-V*) characteristic of solar cells is usually based on the two-diode model, which regards a homogeneous current flow. Due to the distributed character of the series resistance this assumption does not hold for high current densities and leads, beside some other well-known departures from the superposition principle, to two different sets of two-diode parameters describing the recombination and series resistance effects in the dark and under illumination. In this contribution a 1-dimensional model is used for the evaluation of the spatial current distribution and results in a current-dependent effective (lumped) series resistance for the different cases of illumination, which is described empirically. By introducing just one additional series resistance parameter it is possible to characterize the dark and the illuminated *I-V* curve with one physically meaningful set of first diode and series resistance parameters. However the second diode parameters as well as the parallel resistance might be influenced by other departures from the superposition principle. Considering this results, we propose a two-diode model with an analytically given current-dependent series resistance, which may describe the dark as well as the illuminated *I-V* characteristic up to large current densities based on one and the same parameter set. This approach is applied to two different solar cells.

Keywords: Characterization; Two-diode model; current-voltage characteristic; simulation; fit

1. Introduction

The electrical properties of silicon solar cells are commonly evaluated by describing the global current-voltage (*I-V*) characteristic with the widely accepted two-diode model. It implies a first diode

* Corresponding author. Tel.: +49(0) 345 5582 692; fax: +49(0) 345 5511 223.
E-mail address: rissland@mpi-halle.mpg.de.

describing the so-called diffusion current and a second diode describing the (depletion region) recombination current. It specifies the solar cell as a homogeneous device with a constant series resistance, which quantifies the voltage drop from the terminal to the p-n junction. Since the series resistance of a solar cell is caused by different effects of the lateral and local current flow, this is actually a poor description [1,2,3]. In particular, the distributed character of the series resistance, which characterizes the voltage drop due to the conductivity of the front grid and/or the emitter, is neglected by this assumption. Even in an ideal solar cell with homogeneous recombination and series resistance parameters, the different current paths lead for high current densities to an inhomogeneous current flow within the device and therefore to deviations from the supposed *I-V* characteristic. The most familiar result of this fact is that the series resistances obtained in the dark and in the illuminated case are different. But even with different constant series resistances it is not possible to describe the different cases with one and the same physically meaningful set of recombination parameters. [3]

The goal of this contribution is to combine the concept of a distributed series resistance with the two-diode model. Thus we will apply a current-dependent series resistance, which was received from a numerical simulation of a solar cell. Empirically obtained analytical expressions describing the current dependence can be simply combined with the two-diode model and enable a description of the dark and illuminated *I-V* characteristic by the same physically meaningful set of recombination and series resistance parameters. This approach is applied to two different solar cells.

2. Experimental details

For a correct interpretation of the series resistance R_s of an evaluated *I-V* curve it has to be ensured that no additional series resistance caused by the contacting is measured. Therefore the sample was measured by a four-probe contact scheme. The solar cell was sucked on a water-cooled measurement chuck providing a homogeneous contact of the rear side, and it was biased by a four quadrant power supply. Each front side busbar is contacted via six spring-loaded pins mounted along a low-ohmic contact rail, which includes additional sense pins contacting the middle of each front side busbar. Also at the rear side contact a sense pin exists. Since a constant sample temperature during the measurement is essential for a correct interpretation of the *I-V* characteristics, the solar cell surface temperature was monitored by an IR-thermometer. Under illumination the temperature of the chuck was decreased until the temperature of the cell reaches 25 °C as in the dark.

3. Simulation

The most common way to interpret the local R_s of a solar cell is to define it by the voltage drop between the local bias and the cell's terminal voltage, divided by the local current density. Unfortunately this approach describes the local voltage distribution only for the used biasing condition correctly, but not for the general case of any biasing condition, since it does not consider the distributed character of the series resistance.

To evaluate the influence of the distributed character of the series resistance, the solar cells has to be investigated at least as a two-dimensional device. Several approaches for imaging the local R_s (e.g. [4,5,6]) have imaged a local effective series resistance, which increases between the busbars and also between the grid lines. Since the variation of R_s from busbar to busbar is stronger than from grid line to grid line, we expect that a one-dimensional model in grid line direction will describe the main contribution of the distributed R_s [3].
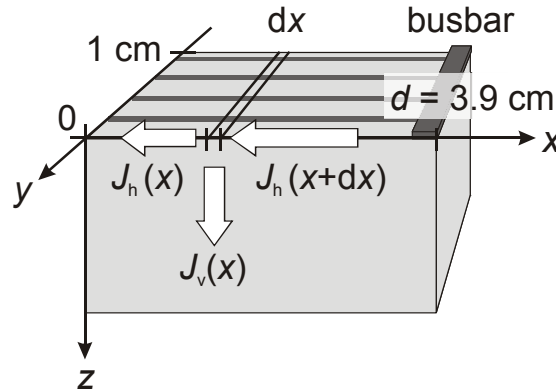
Fig. 1. Investigated symmetry element with J_v being the vertical and J_h the horizontal current density (without illumination). [3]

Since this model is discussed in detail in [3], here just a brief summary of the main ideas will be presented. As for model (B) from [2] we assume a homogeneous series resistance R_{hom} for the vertical current flow (in units of Ωcm^2) in each position x in addition to the distributed resistance. The corresponding symmetry element of our approach is presented in Fig. 1. It contributes the horizontal current flow J_h (in units of A/cm) in a sheet parallel to the grid lines, regarded as an effective sheet resistance ρ_s (in units of $\Omega_\square$), and the vertical current flow J_v (in units of A/cm^2) over the p-n junction, which is described by its saturation current density J_{01} and its ideality factor n_1. Since there is no homogeneous current distribution caused by J_{02} and R_p, these contributions are not considered here.

Starting with an assumed voltage $V(0) = V_0$ we numerically calculate the local voltage and accumulate the current step by step from the middle of the cell to the busbars, ending there with the terminal voltage V and the current I [3]. Repeating this procedure for various V_0 obtains the global $I(V)$ characteristic of the simulated homogeneous solar cell, which can be interpreted according to the assumed recombination parameters.

The distributed series resistance is influenced by the effective sheet resistance ρ_s as well as the geometrical dimension d, representing half the distance between the busbars. The magnitude $\rho_s d^2$, which has the dimension of an area-related resistance, has been called "geometrical resistance" in [1] and "R_{CC}" in [2]. In the following, we will refer to eqn. (1), including the factor 1/3, as the (area-related) "global distributed series resistance" R_{dis} of this cell, since for low currents this resistance simply adds up to the homogeneous resistance.
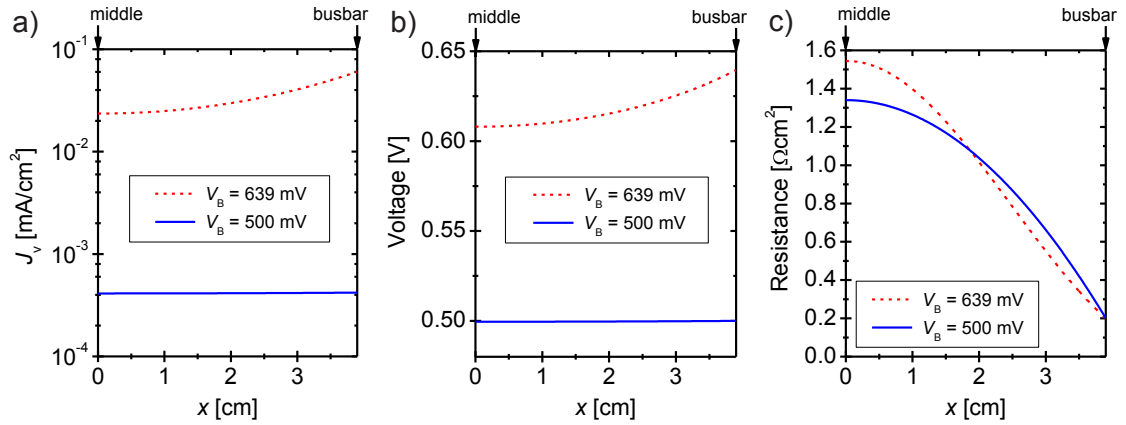
$$R_{dis} = \frac{1}{3}\rho_s d^2 \tag{1}$$

Fig. 2. Vertical current, voltage, and effective series resistance profile from the middle of the cell to a busbar for two bias voltages without illumination. [3]

4. Results

4.1. Current and voltage profiles

Fig. 2 indicates the simulated distribution of the vertical current flow $J_v(x)$ and the local voltage at a typical solar cell with the series resistance parameters $R_{hom} = 0.2$ Ωcm^2 and $R_{dis} = 0.7$ Ωcm^2. We assume $J_{01} = 1.48 \times 10^{-12}$ A/cm^2 and plot the data for the bias of 500 mV and 639 mV without illumination. It is obvious that at 500 mV the current density is still homogeneous, but spatially varies by a factor of almost 3 at 639 mV. At this applied voltage the local voltage decreases by 31 mV from the busbar to the middle of the cell due to distributed series resistance.

The effective local series resistance is calculated by dividing the voltage drop at each position by the local vertical current density $J_v(x)$. For the low current resp. voltage case at 500 mV, the well-known parabolic R_s profile is obtained. In the high current case at 639 mV, the curve follows a clearly different behavior. Due to the changed current paths the resistance in the middle of the cell is higher than for a homogeneous current flow, while near the busbars a lower R_s is calculated. Therefore the main current contribution flows near the busbars, where the voltage drop is still low.

4.2. Current-dependent lumped series resistance

The simulated global *I-V* characteristics can be evaluated by the one-diode model assuming homogeneous current flow, leading to a calculation of the lumped series resistance R_s for each current density J:

$$R(J) = \frac{U - V_T \ln\left(\frac{J + J_{sc}}{J_{01}} + 1\right)}{J} \qquad (2)$$

It has been already shown in [1,3] that the distributed character of the series resistance leads to a current-dependent series resistance, which decreases with increasing current density in the dark and raises under illumination. According to the analytically obtained results of Araújo et al. [1], which just describe the special biasing condition of J_{sc} and V_{oc}, we have derived analytical expressions to fit our numerical simulations for all conditions [3]. This current-dependent series resistance is characterized by the parameters R_{dis} and R_{hom} as well as the current densities J and J_{sc} and the ideality factor n_1. Due to the different current paths it is necessary to differ between the dark and the illuminated case, but the asymptotical limits are consistent to each other. For the dark series resistance $R_s^{dark}(J)$ we obtain:

$$R_s^{dark} = \frac{\theta_{dark}}{\tanh(\theta_{dark})} R_{hom} + \left(\frac{\theta_{dark}}{\tanh(\theta_{dark})} - 1 \right) \frac{n_1 \cdot V_T}{1.6 \cdot J} \tag{3}$$

$$\theta_{dark} = \sqrt{\frac{3 \cdot R_{dis}}{R_{hom} + \dfrac{n_1 \cdot V_T}{1.6 \cdot J}}}$$

This dependence is displayed in Fig. 3 for the two fitted experiment datasets (see next section) as solid lines labeled "Fit R_s^{dark}". The series resistance in the illuminated case can be described by equation (4), which was obtained from an interpolation of the results given by Araújo et al. [1] for the open circuit and short circuit case. Also this dependence is shown in Fig. 3 as dashed lines labeled "R_s^{illum}".

$$R_s^{ill} = \frac{\theta_{ill}}{\tanh(\theta_{ill})} R_{hom} + \left(\frac{\theta_{ill}}{\tanh(\theta_{ill})} - 1 \right) \frac{n_1 \cdot V_T}{J_{sc} - J} + \left(\frac{J}{J_{sc}} \right)^{\beta} \left[\frac{-n_1 \cdot V_T}{J_{sc}} \ln \left(\frac{2\alpha}{\sqrt{\pi} \cdot erf(\alpha)} \right) + \frac{1}{2} R_{dis} \right] \tag{4}$$

$$\theta_{ill} = \sqrt{\frac{3 \cdot R_{dis}}{R_{hom} + \dfrac{n_1 \cdot V_T}{J_{sc} - J}}} \qquad\qquad \alpha = \sqrt{\frac{3 \cdot R_{dis} \cdot J_{sc}}{2 \cdot n_1 \cdot V_T}} \qquad\qquad \beta = 1 + \frac{R_{hom} J_{sc}}{1.5 \cdot n_1 \cdot V_T}$$

4.3. Application to measured I-V characteristics

The above mentioned expressions are used to describe the dark and illuminated characteristic of multicrystalline silicon solar cells with a physically meaningful set of parameters. We investigate two cells of different size to characterize the distributed character of the series resistance. Sample A is a 156×156 mm sized and sample B is 125×125 mm wide. Both samples have an H-patterned grid design with two busbars.

First, we will fit the dark *I-V* characteristic to our variable resistance model. Therefore the low current part of the characteristic (up to 2 mA/cm^2) is fitted to the two-diode model in the conventional way. The fitting procedure used here was developed by Suckow et al. [7] and is freely available [8]. The series resistance in that current regime is still almost constant (see Fig. 3) and represents $R_{dis}+R_{hom}$. Since the general influence of R_s is weak, there is a large uncertainty, but the parameters J_{01}, J_{02}, n_2, and R_p are obtained with sufficient accuracy. The ideality factor n_1 of the first diode has to be assumed. Knowing these dark current parameters, the open circuit voltage can be evaluated, which is independent from R_s. Doing this with our data assuming $n_1 = 1$, V_{oc} of sample A appears to be 2 mV smaller than measured.

This deviation may be caused by an injection-dependent lifetime in the bulk, which leads to an ideality factor of the diffusion current slightly larger than unity [9].Using $n_1 = 1.02$ in the two-diode fit results in the correct V_{oc}-value simulated from the dark I-V curve parameters. For the sample B the assumed n_1 remains unity. Another possibility to achieve the two-diode parameters without the influence of R_s is a direct fit to a measured Suns-V_{oc} curve, which was not available for the authors.

Knowing the two-diode parameters enables to calculate the diode voltage $V_{diode}(J)$ for all current densities $J > 2$ mA/cm^2 and thus to evaluate the current-dependent lumped series resistance according to:

$$R_s(J) = \frac{V_{dark}(J) - V_{diode}(J)}{J} \tag{5}$$

Fig. 3 shows the results of this procedure for the two samples together with the corresponding fitted dependencies expected from (3). The optimum fit delivers for sample A: $R_{hom}^{(A)} = 0.13$ Ωcm^2 and $R_{dis}^{(A)} = 0.83$ Ωcm^2 and for sample B: $R_{hom}^{(B)} = 0.03$ Ωcm^2 and $R_{dis}^{(B)} = 0.66$ Ωcm^2. Regarding the different geometrical parameter $d^{(A)} = 3.9$ cm and $d^{(B)} = 3.1$ cm results in similar effective sheet resistances $\rho_s^{(A)} = 0.163$ $\Omega_\square$ and $\rho_s^{(B)} = 0.201$ $\Omega_\square$. The corresponding R_s-values for the low current case and for $J = J_{sc}$ according to eqn. (3) and (4) are summarized in Tab. 1.

The next step is to fit the illuminated characteristic. Since we have no access to an AM 1.5 cell tester, we measure the illuminated I-V characteristics by homogeneous irradiation of monochromatic (850 nm) light, with the intensity chosen to match the value of J_{sc} given by the producer of the cell. The measured I-V characteristic is corrected by the R_s^{ill} according to the fitting parameters obtained from the dark I-V characteristic. For evaluating the illuminated characteristics it is useful to display them logarithmically in the style of a dark characteristic by subtracting J_{sc} from all illuminated current values, as it has been done also e.g. by Araújo [1]. This R_s-corrected illuminated I-V characteristic is plotted in Fig. 4 together with the simulated J_{sc}-V_{oc}-curve and the measured dark I-V characteristic for both samples.
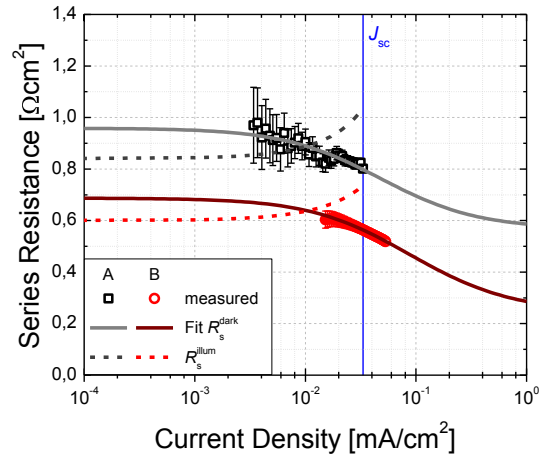

Fig. 3. Evaluated current-dependent dark series resistance R_s^{dark} form the measured dark I-V curves of sample A and B and corresponding illuminated series resistance R_s^{illum} ($n_1^{(A)} = 1.02$, $n_1^{(B)} = 1.0$).

Table 1. Dark and illuminated lumped series resistance obtained from Fig. 3 for current density $J = 0$ and $J = J_{sc}$.

	Sample A		Sample B	
	$J = 0$	$J = J_{sc}$	$J = 0$	$J = J_{sc}$
R_s^{dark} [Ωcm^2]	0.96	0.71	0.69	0.56
R_s^{ill} [Ωcm^2]	0.84	1.04	0.60	0.73

It is obviously visible that the values of the R_s-corrected illuminated *I-V* characteristic correspond quite well with the J_{sc}-V_{oc} curve in high current regime. The fit parameters of these curves are presented together with the parameters obtained from the dark *I-V* fit in Tab. 2. Here, in addition to the results of the procedure regarding R_{dis} described in this contribution, also curve fitting results assuming a constant R_s are presented, labeled as "$R_{dis} = 0$". It is visible already in Fig. 4 that in Sample B the second diode (depletion region recombination) current is much higher than in Sample A. In the analysis regarding R_{dis}, the diffusion current densities J_{01} of both samples coincide for the dark and the illuminated case, but the recombination current density J_{02} as well as n_2 and R_p differ. This is due to well-known departures from the superposition principle, which had been described already in [10]. One of the departures described in this paper appears for significant recombination in the bulk and/or at the backside, which might be caused here by the recombination at the Al back contact and in the multicrystalline bulk. According to [10] this leads to an additional current-dependent recombination path, which may be described by an additional contribution to the parallel conductance and/or to the second diode (J_{02}, n_2). Since this effect depends on the current density, it becomes negligible at low illumination intensity and is therefore not measurable with the suns-V_{oc} method. By the way, this additional recombination path under illumination is the reason why in PL imaging always the PL image under short circuit has to be subtracted to account for the "diffusion-limited carriers" [4]. Hence, if this departure from the superposition principle holds (which should be the case for all industrial solar cells), it cannot be expected that the two-diode evaluation of illuminated characteristics leads to the same values of J_{02}, n_2 and/or R_p as the evaluation of the dark characteristic. Fitting the dark and illuminated characteristic with constant R_s ($R_{dis} = 0$) results for both samples in almost the same R_s, but very different J_{01}. This is not physically meaningful.
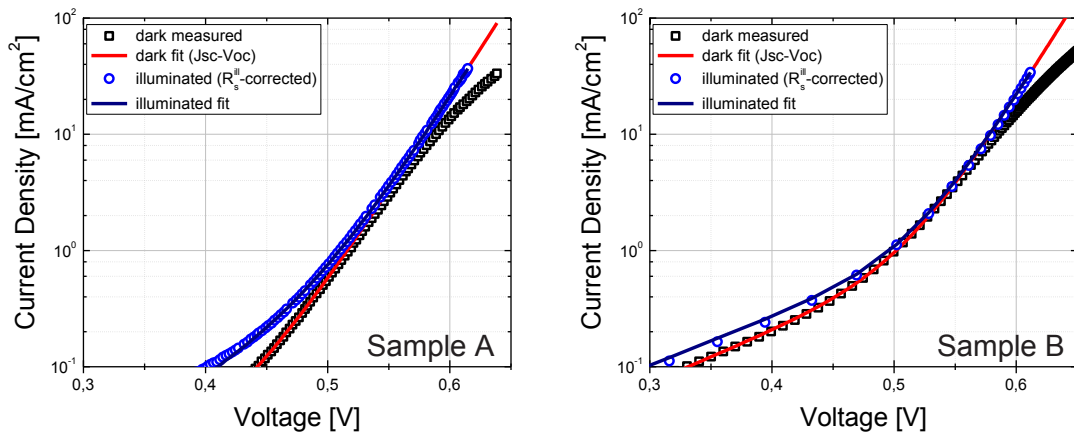

Fig. 4. Measured dark *I-V* characteristic and R_s-corrected illuminated *I-V* characteristic (1.0 suns) in comparison with the R_s-corrected dark *I-V* characteristic (J_{sc}-V_{oc}).

Table 2. Two-diode parameters obtained from dark and illuminated *I-V* characteristics with constant and current-dependent R_s.

	Sample A				Sample B			
	dark	illuminated	dark	illuminated	dark	illuminated	dark	illuminated
R_s [Ωcm^2]	$R_{dis} = 0$	$R_{dis} = 0$	$R_{dis} = 0.83$	$R_{dis} = 0.83$	$R_{dis} = 0$	$R_{dis} = 0$	$R_{dis} = 0.66$	$R_{dis} = 0.66$
	$R_{hom} = 0.91$	$R_{hom} = 0.92$	$R_{hom} = 0.13$	$R_{hom} = 0.13$	$R_{hom} = 0.52$	$R_{hom} = 0.48$	$R_{hom} = 0.03$	$R_{hom} = 0.03$
J_{01} [A/cm^2]	1.53e-12	1.28e-12	2.33e-12	2.28e-12	1.43e-12	1.22e-12	1.48e-12	1.48e-12
n_1	1.0	1.0	1.02	1.02	1.0	1.0	1.0	1.0
J_{02} [A/cm^2]	7.60e-9	2.99e-8	7.00e-9	2.37e-7	3.32e-6	4.79e-8	3.78e-6	7.20e-6
n_2	2.0	2.0	2.0	2.70	3.78	2.0	3.91	4.3
R_p [Ωcm^2]	39215	22759	38502	8264540	108076	3245	222311	200000

5. Discussion

Applying the two-diode model with a fixed series resistance enables to fit the dark and illuminated *I-V* characteristic of crystalline silicon solar cells separately, but leads, at least if high currents are employed, to two different sets of two-diode parameters for the illuminated and dark case. We have already discussed here that this deviations are caused by two different reasons. The high current regime of both characteristics is influenced by the distributed character of the series resistance and leads, if this is not regarded, to different values of R_s and J_{01}. We regarded this by the introduction of the additional global distributed series resistance R_{dis}. At low currents (below 0.1 I_{sc}) R_{dis} simply adds to the homogeneous series resistance R_{hom} for the dark case. At high currents (above 0.1 I_{sc}) R_{dis} leads to current-dependent effective lumped series resistance and may be described by the empirical formulas (3) and (4) already given in [3], which also consider R_{hom}.

In contrast to that, the deviations between dark and illuminated characteristics in the low voltage regime are due to departures from the superposition principle described by Robinson et al. [10]. This departure is caused by an additional current-dependent bulk recombination under illumination and is due to the higher minority carrier concentration under illumination and under current extraction than in the dark, considering the same bias. It is obvious that this effect also depends on the illumination intensity and becomes negligible for low intensities. The application of the two-diode model to illuminated *I-V* characteristics usually results in significantly increased values of J_{02} and n_2, and may also affect the R_p value. Therefore it cannot be expected that the second diode and R_p-parameter match for the dark and the illuminated characteristic at 1 sun. However, the values of R_s and J_{01} should be the same in the dark and under illumination for the consistent description of a solar cell, which is the case for our current-dependent R_s approach introduced here.

6. Conclusion

The two-diode model does not allow a consistent description of the dark and the illuminated *I-V* characteristic even if two different fixed series resistances are assumed. Regarding the distributed character of the series resistance by defining one new parameter R_{dis} enables to specify the dark and the illuminated *I-V* characteristic by a single set of diffusion current and R_s parameters. The additional R_{dis} leads, according to a numerical simulation, to a current dependency of the lumped series resistance. Two different multicrystalline solar cells are investigated here to examine this new approach. Firstly the low

current regime of the dark characteristics is fitted to a conventional two-diode model with a constant R_s. This leads to reliable values of J_{01}, J_{02}(dark), n_2(dark), and R_p(dark). The ideality factor n_1 may be adjusted to a value slightly above unity until the simulated suns-V_{oc} characteristic considering these parameters matches the measured V_{oc} at J_{sc}. This might be caused by an injection-level dependent lifetime in the multicrystalline silicon solar cells. The current-dependent dark series resistance is evaluated by a comparison of the suns-V_{oc} with the measured dark characteristic and is fitted by the analytical expressions (3) and (4) developed in [3]. In the cases introduced here the series resistance of the larger solar cell (A) has a higher distributed resistance than the smaller one (B), which is mainly caused by the longer current paths from the area to the terminals. The resulting values of R_{dis} and R_{hom} are used to correct the illuminated *I-V* characteristic, which can be fitted by the two-diode model afterwards. This leads to the same values for J_{01}, but different values of J_{02}(ill.), n_2(ill.) and, eventually also R_p(ill.). This discrepancy is caused by departures from the superposition principle [10].

Acknowledgements

References

[1] Araújo GL, Cuevas A, Ruiz JM. The effect of distributed series resistance on the dark and illuminated curent-voltage characteristics of solar cells. *IEEE Transactions on Electron Devices* 1986;**33**:391-401.

[2] Fischer B, Fath P, Bucher E. Evaluation of solar cell *J*(*V*)-measurements with a distributed series resistance model. In: *Proceedings of the 16th European Photovoltaic Solar Energy Conference*, Glasgow; 2000, p. 1365-68.

[3] Breitenstein O, Rißland S. A two-diode model regarding the distributed series resistance. *Solar Energy Materials and Solar Cells* 2013;**113**:77-86.

[4] Trupke T, Pink E, Bardos RA, Abbott MD. Spatially resolved series resistance of silicon solar cells obtained from luminescence imaging. *Applied Physics Letters* 2007;**90**:093506.

[5] Haunschild J, Glatthaar M, Kasemann M, Rein S, Weber ER. Fast series resistance imaging for silicon solar cells using electroluminescence. *Physica Status Solidi (RRL)* 2009;**3**:227-9.

[6] Breitenstein O, Khanna A, Augarten Y, Bauer J, Wagner J-M, Iwig K. Quantitative evaluation of electroluminescence images of solar cells. Physica Status Solidi (RRL) 2010;**4**:7-9.

[7] Suckow S, Pletzer TM, Kurz H. Fast and reliable calculation of the two-diode model without simplifications. *Progress in Photovoltaics: Research and Applications* 2012: accepted; DOI: 10.1002/pip.2301.

[8] Suckow S. (2012), "2-Diode Fit", https://nanohub.org/resources/14300.

[9] Macdonald D, Cuevas A. Reduced fill factors in multicrystalline silicon solar cells due to injection-level dependent bulk recombination lifetimes. *Progress in Photovoltaics: Research and Applications* 2000;**8**:363-75.

[10] Robinson SR, Aberle AG, Green MA. Departures from the principle of superposition in silicon solar cells. *Journal of Applied Physics* 1994;**76**:7020-30.